Nature Communications

https://doi.org/10.1038/s41467-026-73533-y

Article in Press

Disinfection of hospital sink drains enriches pseudomonadota and efflux pump-mediated antibiotic resistance in reestablished biofilms

Received: 17 October 2025

Accepted: 6 May 2026

Cite this article as: Bowie, K.R., Luhung, I., Burke, T.R. *et al.* Disinfection of hospital sink drains enriches pseudomonadota and efflux pump-mediated antibiotic resistance in reestablished biofilms. *Nat Commun* (2026). https://doi.org/10.1038/s41467-026-73533-y

Kate R. Bowie, Irvan Luhung, Taylor R. Burke, Scott C. Roberts, Richard A. Martinello, Mark Gerstein, Jordan Peccia & Hannah G. Healy

Disinfection of Hospital Sink Drains Enriches Pseudomonadota and Efflux Pump-Mediated Antibiotic Resistance in Reestablished Biofilms

Kate R. Bowie[1,2], Irvan Luhung[1], Taylor R. Burke[1], Scott C. Roberts[3,4], Richard A. Martinello[3,4,5], Mark Gerstein[1,6,7,8]*, Jordan Peccia[1]*, Hannah Greenwald Healy[9]*

1. Department of Chemical and Environmental Engineering, Yale University, New Haven, CT, USA
2. Department of Molecular Biophysics and Biochemistry, Yale University, New Haven, CT, USA
3. Department of Internal Medicine, Section of Infectious Diseases, Yale School of Medicine, New Haven, CT, USA
4. Infection Prevention, Yale New Haven Health, New Haven, CT, USA
5. Department of Pediatrics, Yale School of Medicine, New Haven, CT, USA
6. Program in Computational Biology & Bioinformatics, Yale University, New Haven, CT, USA
7. Department of Computer Science, Yale University, New Haven, CT, USA
8. Department of Statistics & Data Science, Yale University, New Haven, CT, USA
9. Harvard T.H. Chan School of Public Health, Harvard University, Boston, Massachusetts

*Correspondence to:
Hannah Greenwald Healy, PhD
Email: hannahhealy@hsph.harvard.edu

Jordan Peccia, PhD
Email: jordan.peccia@yale.edu

Mark Gerstein, PhD
Email: pi@gersteinlab.org

Abstract

Antimicrobial resistant pathogens and associated infections represent major public health threats affecting healthcare facilities, with sink drain biofilms serving as reservoirs for many of these bacteria. Despite attempts at sink drain biofilm disinfection and removal, drain biofilms inevitably regrow, and disinfection may shape the returning microbial communities and their resistance profiles. We applied culture-based and metagenomic approaches to study these drain disinfection effects on microbial community abundance, taxonomy, and antimicrobial resistance in operational hospital sinks. Drain biofilms regrew to baseline densities in approximately four days. Regrown biofilms contained more viable carbapenem-resistant bacteria and were dominated by Pseudomonadota, including *Cupriavidus* and *Pseudomonas*. Long-read sequencing revealed an increase in multidrug efflux pump genes after disinfection, which confer broad resistance to antibiotics and disinfectants. This work provides mechanistic insights into how disinfection influences sink drain biofilm ecology and the enrichment of antimicrobial resistance, with implications for infection prevention strategies in healthcare environments.

Introduction

Multi-drug resistant hospital-acquired infections (HAIs) cost an estimated $1.9 billion in the United States annually,[1] and treatment is increasingly more complex with rising antimicrobial resistance (AMR). Recent research has produced substantial evidence supporting sink drains as reservoirs of antimicrobial resistant bacteria (ARB), and drain ARB have been linked to AMR HAI outbreaks,[2–7] with established pathways of dispersion from drains into hospital rooms during sink use.[8] Sink drains promote the persistence of ARB through the growth of dense biofilm formation, which fosters close microbial interactions and facilitates horizontal gene transfer, a process by which bacteria can exchange antibiotic resistance genes.[9] Environmental investigations into sink drain biofilms have identified ARB, such as multidrug-resistant *Pseudomonas aeruginosa*, *Cupriavidus pauculus*, *Acinetobacter baumannii*, and *Stenotrophomonas maltophilia,*[8] many of which are listed as priority AMR pathogens by the World Health Organization (WHO) and United States Centers for Disease Control and Prevention (CDC).[10,11] Given that healthcare sink drains play a role as reservoirs for priority ARB, interventions that prevent the growth of resistant pathogens in sink drains are critically needed. Equally important is understanding how such interventions alter the microbial ecology of drain biofilms, since biofilm dynamics and taxonomic composition directly influence the persistence and dissemination of antimicrobial resistance.

Drain disinfection is met with the challenge of ensuring sufficient contact time with vertical pipe walls. Recent foaming disinfectants have addressed that issue and have been gaining popularity in healthcare settings; however, guidance on application frequency and evidence of impacts in real-world settings is lacking. A recent study on one such product demonstrated efficacy against a variety of bacterial, yeast, and viral pathogens, and reduced overall bacterial abundance when applied to real sink drain biofilms every 4-5 days.[12] Other studies evaluating foaming disinfectants applied between one and five times per week demonstrated decreases in opportunistic pathogens, such as *Pseudomonas aeruginosa*, *Stenotrophomonas maltophilia*, and *Acinetobacter* spp., though strain-level genomic analyses revealed some pathogens can persist or re-establish post intervention.[13,14] Despite temporary success in reducing microbial abundance in drains with typical disinfectants,[15,16] previous work has demonstrated that biofilms can reestablish relatively quickly and that disinfection in other contexts can preferentially select for antibiotic resistant organisms.[17,18] These interventions are typically evaluated only in terms of bulk microbial load reduction, leaving their ecological and resistance-related impacts poorly understood. Addressing this gap is essential because interventions may not simply eradicate pathogens but instead, lead to regrowth that reshapes the microbial ecology and AMR of drain biofilms. Whether disinfection reduces clinically relevant resistance genes, selects for stress-tolerant organisms, or reshapes taxonomic diversity in sink drain biofilms remains largely unknown.

Here, we used culture-based assays in combination with short- and long-read metagenomics to investigate how the microbial communities in hospital sink drain biofilms respond to treatment with a foaming disinfectant with active ingredients of hydrogen peroxide, octanoic acid, and peroxyacetic acid. We evaluated the sink drain biofilms of 19 operational sinks at Yale New Haven Hospital over 36 days. Biofilms were sampled prior to disinfection to identify baseline abundance and taxonomy, then sampled at several timepoints for three weeks after treatment (Figure 1). We examined the viability and abundance of the microbial community through culture using agar with and without antibiotics to measure total and carbapenem-resistant bacteria (n = 156 samples). To better characterize the community members of the sink biofilms, we utilized short-read metagenomic sequencing (n = 119

samples). Lastly, long-read sequencing was applied to resolve the host context of antibiotic resistance genes (ARGs), providing insight into which bacteria carried resistance determinants and whether they were on chromosomes or mobile elements (n = 24 samples). This overall approach allowed us to link changes in resistance phenotypes to genomic mechanisms and taxonomic dynamics, providing insight into how interventions may unintentionally favor reduced microbial diversity and broad-spectrum resistance in critical healthcare reservoirs.

Results

Disinfection reduced bacterial abundance followed by regrowth that enriched for carbapenem-resistant bacteria

We evaluated the sink drain biofilms of 19 unique sinks (12 treated, 7 untreated) on a hematology and oncology unit that typically cares for patients with hematopoietic stem cell transplants at Yale New Haven Hospital. Of the treated sinks, six sinks were located in patient rooms while the other six were located in hallways outside patient rooms, but still within the clinical unit. In the 156 samples collected, we assessed abundance of viable total bacteria and carbapenem-resistant bacteria by counting colony forming units (CFU) of homogenized samples spread onto ChromAgar Orientation plates (no carbapenem) and ChromAgar KPC (with carbapenem) plates, respectively. We designated three phases based on bacterial abundance and growth patterns surrounding treatment: baseline bacterial abundance before treatment ('Before'), reduced bacterial abundance following treatment ('After'), and regrowth period of bacterial abundance returning to at least baseline levels ('Regrowth', Figure 1). At baseline ("before" disinfection), the median drainpipe surface loading of total bacteria was $1.2\times10^7\pm 9.2\times10^6$ CFU/cm^2, while the median of carbapenem-resistant bacteria was $2.2\times10^6\pm 6.7\times10^6$ CFU/cm^2. The log-reduction values across sinks ranged from 0 to 4.2 log-reduction in colony-forming units immediately following disinfection treatment, with median log-reduction of approximately 1.5 (Figure 2, with carbapenem: median 11.6 million CFU/cm^2 versus 587,000 CFU/cm^2; without carbapenem: median 2.2 million CFU/cm^2 versus 74,800 CFU/cm^2). Immediately following disinfection treatment, many samples had no detectable colonies (with carbapenem: n = 3, without carbapenem: n = 11). Biofilms began to regrow after the single drain treatment, reaching the initial bacterial abundance after four days (median of 12.5 million CFU/cm^2 and 15.3 million CFU/cm^2 for carbapenem positive and negative plates, respectively). Although total bacterial abundance increased during the regrowth phase relative to baseline, it was not significantly different from that of the seven untreated control sink drains, suggesting that external factors (e.g., temperature, relative humidity, usage patterns) contributed to the observed increases across all sinks (Figure 2C).

Disinfection treatment led to elevated carbapenem-resistant bacteria in the regrowth phase relative to baseline. The resistant fraction of bacteria was highest in the regrowth phase (median 50.0% IQR [19.2%, 81.8%], p = 0.05) and lowest before treatment (median 15.7% IQR [6.6%, 43.8%], after: median 26.1% IQR [5.8%, 61.5%]). The abundance of carbapenem-resistant bacteria in treated sinks was significantly higher than in the untreated sinks during the regrowth phase (Figure 2D). These trends of initial reduction of bacterial abundance post-treatment followed by regrowth with enriched antimicrobial resistance were consistent across both hallway and patient-room sinks (Supplementary Figure 1).

Treatment led to enrichment of *Pseudomonas* and *Cupriavidus* and decreased diversity in reestablished biofilms

To evaluate the impact of treatment and regrowth on microbial community taxonomy, we sequenced a total of 123 samples via Illumina short-read sequencing, which included samples from three collection days in each experimental phase, two negative controls, two positive controls, and seven untreated control sinks (Supplementary Table 1). The sink drain biofilms were taxonomically diverse, consisting of 41 assigned phyla and 1,648 assigned genera (Figure 3A). The four most abundant phyla in the sink drain biofilms were *Pseudomonadota*, *Actinomycetota*, *Bacteroidota*, and *Bacillota*. The top five most abundant genera across all experimental phases were *Cupriavidus*, *Pseudomonas*, *Sphingobium*, *Novosphingobium*, and *Comamonas* (Figure 3A, Supplementary Figure 2), which are commonly detected in hospital water systems.[19–21]

The biofilm microbial community that regrew after disinfection treatment was significantly different from the biofilm community before disinfection treatment (Supplementary Figure 3). *Cupriavidus* and *Pseudomonas* were the predominant taxa in the regrowth phase (Figure 3A), which coincided with a significant decrease of alpha diversity after treatment that persisted during the regrowth phase (Inverse Simpson index, $p = 0.00003$, Kruskal-Wallis, Figure 3C, Figure 3E; Supplementary Table 2). Additionally, we found a significant difference in the beta diversity of the microbial communities when comparing before treatment to the regrowth phase (Bray-Curtis, $p < 0.001$, PERMANOVA, Supplementary Figure 4), but it should be noted that there were significant differences in the reads generated from each experimental phase ($p = 1.74 \times 10^{-5}$, Kruskal-Wallis, Supplementary Figure 5). To assess whether these compositional shifts exceeded those from random ecological drift, we applied a Raup-Crick (RC) null model based on Bray-Curtis dissimilarity. RC values both within and across phases were generally high (>0.95), consistent with deterministic structuring. Next, we investigated the specific taxa contributing to the overall composition changes by examining differentially abundant taxa throughout the three experimental phases (Figure 3F, Supplementary Table 3). Our analysis revealed that *Cupriavidus, Ralstonia*, *Pseudomonas*, and *Stenotrophomonas* were significantly higher during regrowth, while *Burkholderia* was significantly lower (MaAsLin3, $p < 0.05$, Figure 3F, Supplementary Table 3). *Moritella* was the genus with the lowest p-value ($p = 3.42 \times 10^{-302}$, mean relative abundance of 6.78×10^{-7}), although likely a statistical artifact and contaminant, as *Moritella* has not been documented to be in hospitals, pipes, nor near humans,[22] and was removed from the analysis.

Genera containing primary and opportunistic pathogens were consistently detected in sink drain biofilm microbial communities, with higher overall abundance of pathogen-containing genera after treatment. Using Chan Zuckerberg ID's 2024 pathogen list,[23] we found 73 unique genera in our sink drain biofilm communities (Supplementary Table 4). There was a median of 69 pathogen-containing genera (IQR: 67, 70 pathogens) detected per sink drain biofilm and no significant differences in number detected across the experimental phases. The top 5 pathogen-containing genera detected were *Pseudomonas*, *Stenotrophomonas*, *Mycobacterium*, *Enterobacter*, and *Mycolicibacterium*, all associated with water systems.[24] The relative abundance of all pathogens was significantly higher directly after treatment and in the regrowth phase compared to before treatment ($p=0.03$, Kruskal-Wallis, Supplementary Figure 6).

Sink location shaped biofilm community composition and response to treatment

Sink location (in a patient room versus in a hallway) can influence its use, where mechanistic factors including temperature, relative humidity, and nutrient inputs can impact microbial community composition.[21,25] The beta diversity between hallway and patient sink drain biofilms were significantly different at each experimental phase, indicating location impacted community composition, and that room type should be incorporated as a covariate into downstream analysis (Bray-Curtis, p = 0.001, Supplementary Table 5). We found no significant differences in reads generated by sample type (i.e., hallway or patient room sinks, Supplementary Figure 12). Although patient and hallway sinks shared the same top five phyla and same top genus, *Cupriavidus* (Figure 3C), hallway sinks maintained significantly higher relative abundance of *Pseudomonas* over the sampling period (Figure 3D, p = $1.6x10^{-13}$, Kruskal-Wallis). In certain patient sinks there were large blooms of *Pseudomonas* during regrowth; however, the majority of patient sinks contained *Pseudomonas* at low levels (<5%), as shown by the distribution in Figure 3D. These location-specific differences likely reflect variations in sink use, including both frequency and type of activity, which in turn may influence the reestablished biofilm.

Metagenomic shotgun sequencing revealed decreased overall abundance of antibiotic resistance genes through treatment phases

In drain biofilm metagenomes, the five most abundant ARGs present were *adeF, qacG, qacJ, ANT(2)-Ia,* and *OXA-2*. These genes facilitate antibiotic resistance through different mechanisms, either by encoding efflux pumps with resistance to both antibiotics and disinfectants (adeF, qacG, qacJ),[26,27] enabling aminoglycoside modifications (*ANT(2)-Ia*),[28] or producing β-lactamases with ability to degrade carbapenems (*OXA-2*).[29] The combined median reads per kilobase million (RPKM) of all ARGs in the sink drain biofilms was 2646.6 (IQR: 2036.0, 3312.5 RPKM). Although the culture results demonstrated higher phenotypic carbapenem resistance in reestablished biofilms, overall ARG abundance was significantly lower during regrowth compared to both before treatment and after treatment (p = 0.005, Kruskal-Wallis, Figure 4A). Consistent with the decrease in ARG abundance, ARG alpha diversity was also significantly lower during regrowth compared to before treatment (Shannon p = 0.03; Inverse Simpson p = 0.01, Kruskal-Wallis, Supplementary Figure 7B-C), suggesting that regrowth was characterized by a limited set of ARGs rather than recovery of a diverse resistome. Carbapenem-resistance genes (median: 95.5 RPKM; IQR: 54.7, 197.2 RPKM) followed similar trends to overall ARG abundance, with lower abundance during the regrowth phase compared to both before and after disinfection treatment (p = 0.001, Kruskal-Wallis, Supplementary Figure 8).

Disinfection treatment enriched bacteria with chromosomal antibiotic resistance genes

Long-read sequencing enables the contextualization of antibiotic resistance genes in host bacteria, lessening the likelihood of detecting ARGs from free DNA fragments not associated with live or pathogenic bacteria.[30] We sequenced biofilms from all treated sink drains using PacBio long-read sequencing from two collection dates: before disinfection treatment (day 8, n=12) and during regrowth (day 29, n=12) and analyzed only complete metagenome assembled genomes (MAGs). Between 31.3% and 75.5% of the sequenced base pairs per sample were used to construct MAGs (mean 56.8% ±12.7%). We detected no significant differences in the number of MAGs recovered from samples before or after treatment (mean 11.7 ± 4.8 vs 10.3 ± 1.9, respectively). Within these MAGs, we detected 96 unique ARGs belonging to 27 different drug classes and categorized into 6 distinct

resistance mechanisms (Supplementary Table 6). We annotated an average of 3.5 ± 3.6 ARGs per MAG, including the 9.1% of MAGs without any ARGs. The top 5 most abundant ARGs by relative abundance were *adeF*, *vanT gene in vanG cluster*, *ArnT*, *acrB*, and *mdtB*, which differ from our short-read shotgun metagenomic results beyond the most abundant ARG (*adeF*).

The relative abundance of MAGs carrying ARGs increased significantly after disinfection treatment (Figure 4B), despite no significant change in the total number or ARGs (Supplementary Figure 9, $p > 0.05$), indicating an enrichment of antibiotic-resistant bacteria (Figure 4B). Of the MAGs containing ARGs, we found *Cupriavidus pauculus* and *Pseudomonas_E glycinae* to be the most abundant species, followed by *Phytobacter diazotrophicus* and *Elizabethkingia bruuniana*, all of which have been reported to cause nosocomial infectious except for *Pseudomonas_E glycinae* (Supplementary Figure 10).[19,31–33]

We found carbapenemases to be rare and detected them in only four species during the regrowth phase (Figure 4C, Supplementary Table 7). As previous work has demonstrated that carbapenemases are rarely chromosomal and are primarily located on plasmids,[34] we extended our analysis from only MAGs to also include plasmids. We took all sequences outside of the MAGs and classified them as chromosomal or plasmid, then annotated with ARGs similar to our previous analysis. We found each sample had a median of 436.5 plasmids (IQR: 260.8, 749.3). However, there was no significant change in the number of plasmids from before treatment to the regrowth phase ($p = 0.16$, Figure 4E). Likewise, we found no significant difference in the proportion of plasmids carrying carbapenemases before and after treatment ($p = 0.24$, Figure 4F). Together these observations highlight that mechanisms beyond plasmid-borne carbapenemases, or carbapenemases in general, likely underpin phenotypic resistance in hospital sink drain biofilms following disinfection treatment.

Multi-drug efflux pumps dominated antibiotic resistance in sink drain biofilms after disinfection treatment

The majority of ARGs in the sink drain biofilms were associated with efflux pumps, which can confer low-level, broad-spectrum resistance. Overall, 83.7% of MAGs and 77.9% of species contained at least one ARG classified as an efflux pump. Both the percent of MAGs with efflux pumps and percent of species with efflux pumps increased significantly after treatment ($p=0.03$, $p = 0.008$ respectively). This pattern aligns with the phenotypic increases in carbapenem-resistant bacteria observed in culture, despite the low abundance of canonical carbapenemases.[35] The efflux pump gene *adeF* was highly prevalent and detected across nearly all species, suggesting it may be a core gene in these biofilms, however there was no significant increase after disinfection treatment (Figure 4D**,** $p = 0.24$, two-sided Wilcoxon Rank Sum). Several efflux-associated ARGs, including the *sme* operon genes (*smeD, smeE, smeF, smeA, smeR*), showed apparent increases across MAGs following disinfection (Figure 4D), though paired Wilcoxon tests did not reach statistical significance for these genes. In contrast, the efflux regulator *Pseudomonas aeruginosa soxR* was significantly more prevalent during regrowth ($p = 0.01$, Paired two-sided Wilcoxon test, Figure 4D). This finding was confirmed in the shotgun metagenomic data, where *soxR* abundance differed significantly across growth phases ($p = 1.4 \times 10^{-8}$, Kruskal-Wallis, Supplementary Figure 11B)**.** However, when examining overall efflux pump RPKM in the shotgun data, no significant differences were observed across growth phases (Supplementary Figure 11A), suggesting that the enrichment may be specific to certain efflux regulators rather than the entire efflux gene set.

Discussion

Effective infection prevention approaches are an essential component of patient care. Hospital sink drains frequently harbor biofilms, which serve as established reservoirs of pathogens and have been implicated in HAIs.[2–4] The effects of sink drain disinfection as a means for controlling biofilm growth remains unclear, and evidence supporting its use is limited. In this study, we investigated how a disinfectant for drain biofilms influenced the microbial communities in 12 treated hospital sink drains. Through culturing, we found that disinfection treatment effectively disrupted the biofilm communities and temporarily decreased microbial load (Figure 2, “after”). Despite all sinks being the identical model, there was variability in disinfection efficacy, with viable cell count reductions ranging from 1-2 log, likely due to biofilm heterogeneity. Organic matter can accumulate over time, sometimes clogging drains, which would likely require several treatments or physical means to remove. After treatment, bacterial communities regrew to baseline abundance in approximately four days. These findings parallel prior work demonstrating that repeated disinfection at 4–5 day intervals is required to maintain long-term reduction of biofilm biomass.[12]

The use of the disinfectant resulted in a strong selective pressure to the biofilm microbial communities that reduced diversity and enabled a few taxa to dominate. The metagenomic shotgun sequencing results revealed major compositional changes to the biofilm that consisted of decreased alpha diversity and enrichment of *Cupriavidus* and *Pseudomonas,* which are genera containing clinically relevant species.[19,36,37] A previous study involving the application of peracetic acid disinfectant to sink drain biofilms demonstrated that application resulted in a significant increase in *Pseudomonas spp*. during regrowth and a continued presence of antibiotic-resistant organisms in the drains, agreeing with our results.[38] Long-read sequencing further resolved enriched taxa in our study, identifying *Cupriavidus* as *C. pauculus* while the dominant *Pseudomonas* showed 95.82% average nucleotide identity to *Pseudomonas_E glycinae*, a species previously documented only in soybean rhizospheres.[33] This average nucleotide identity value suggests the recovered MAGs represent a distinct, sink-adapted species within the *P. glycinae* complex. Members of *Pseudomonas* produce extracellular polymeric substances (EPS) which promote biofilm formation and can inhibit fungal growth,[39] features that may provide a competitive advantage within the sink drain environment. The concurrent dominance of *Cupriavidus* and *Pseudomonas* likely reflects both intrinsic tolerance to disinfectants and their ability to recolonize niches exposed by the disruption of extracellular matrix material.[36,40] Moreover, *C. pauculus* has recently been recognized as an emerging opportunistic pathogen capable of causing infections in immunocompromised individuals.[19] Future studies could leverage the metagenomics data generated here to investigate functional traits such as EPS production in *C. pauculus* and *Pseudomonas_E glycinae* to provide deeper insight into the mechanisms driving biofilm persistence following disinfection treatment.

Importantly, resistant bacteria became proportionally more abundant as the biofilm regrew after disinfection treatment, with higher overall abundance of resistant bacteria in treated sinks relative to untreated sinks. The significant increase in the fraction of viable carbapenem-resistant bacteria during regrowth underscores the selective pressure exerted by disinfection treatment, raising the possibility

that disinfectant use may favor resistant subpopulations.[17,18] Our long-read sequencing demonstrated increases in the abundance of MAGs with ARGs, and those ARGs were primarily associated with multidrug efflux pumps (Figure 4). Efflux pumps confer low-level multidrug resistance, often providing a survival advantage in biofilm settings where exposure to disinfectants, heavy metals, and other stressors selects for broad stress-tolerance mechanisms.[41] Specifically, we detected the resistance gene *Pseudomonas aeruginosa soxR*, which is a transcription factor that senses and responds to oxidative stress caused by reactive oxygen species,[42] such as those generated by ingredients in disinfectants. *Pseudomonas aeruginosa soxR* was found in a diverse array of taxa, including *Cupriavidus pauculus*, *Pseudomonas_E glycinae*, and *Novosphingobium spp.* (Figure 4C). All hits were classified as 'strict' by CARD, suggesting the presence of true orthologs. Additionally, our results suggest that treatment may have removed extracellular DNA carrying ARGs. We observed a decrease in total ARG abundance and a reduction in plasmids, even as chromosomally encoded ARGs in surviving MAGs increased. This shift implies that disinfectant pressure selectively eliminates mobile resistance elements while favoring taxa with intrinsic, chromosomally encoded resistance systems, further reinforcing the dominance of *Cupriavidus* and *Pseudomonas* after disinfection treatment.

The observed increase in efflux pumps occurred alongside the increase in phenotypic carbapenem resistance, despite no corresponding increase in the carbapenemase genes. Although the culture-based analysis demonstrated an increase in carbapenem-resistant bacteria, short-read shotgun metagenomics unexpectedly revealed an overall decrease in ARGs as well as a decrease in carbapenemase genes. Using our long-read metagenomic sequencing data, we examined both chromosomal ARGs in complete MAGs as well as ARGs on plasmids but found very few carbapenemases. The only carbapenemase we consistently detected was OXA-2, which has been debated in the literature and is not universally recognized as a true carbapenemase.[29,43] These findings were similar to other studies in which carbapenemases were either not detected at all, or in the minority of their cultured bacteria or isolates.[35,44,45] Instead of carbapenemases, we discovered that many MAGs had ARGs encoding multi-drug efflux pumps (Figure 4C). We speculate a potential explanation is the bacteria could have phenotypic carbapenem resistance through the acquisition of multidrug efflux pumps rather than carbapenemases. This notion is consistent with experimental findings where disinfectant pressure promoted efflux pump overexpression,[46] which can in turn result in carbapenem resistance.[47] However, because we did not perform metagenomics on the cultured biofilms and because the metagenomic sequencing data reflects genetic potential as opposed to gene expression, we interpret the efflux-associated enrichment as a plausible but unvalidated mechanism that warrants further investigation.

This research highlights how different methodological approaches can lead to different interpretations of antimicrobial resistance. Culture-based approaches are the norm in clinical settings, whereas sequencing and molecular methods are becoming increasingly common for environmental surveillance. Metagenomic approaches capture all DNA in a sample, including DNA from viable but not culturable bacteria, lysed cells, or extracellular fragments, thus they can capture more of the community but reflect genetic material not necessarily associated with viable bacteria. In this study, culture-based approaches enabled assessment of phenotypic resistance and viability, while sequencing results enabled identification of resistance mechanisms. Long-read metagenomic sequencing, in contrast with short-read metagenomic sequencing, enabled us to place ARGs in genomic context and distinguish those carried on bacterial chromosomes from those on plasmids, which is critical for understanding their potential for horizontal transfer and resistance mechanisms. However, only the fraction of reads

assigned to complete MAGs are included, and simply counting ARGs can be misleading, since not all detected genes are expressed, functional, or relevant under clinical conditions, which has been demonstrated in a number of studies.[48,49] Functional context, expression, and bacterial viability are necessary to link sequencing data to actual resistance phenotypes. Hence, investigators should be aware of tradeoffs, and the answer may be a combination of culture and sequencing-based approaches.

Taken together, hospitals need to balance the short-term need for pathogen removal in drains with long-term consequences of antimicrobial resistance propagation. These results demonstrate the enrichment of Pseudomonadota with broad efflux-mediated resistance has important implications for hospital infection prevention. Efflux pumps not only confer multidrug resistance but may also facilitate persistence under disinfectant pressure, enabling long-term colonization of sink drains. This combination of persistence and resistance maintains a reservoir from which opportunistic pathogens have the potential to disseminate to vulnerable patients. Thus, while disinfection remains a key tool for reducing biofilm biomass, its infrequent or sporadic application may inadvertently select for communities with heightened resistance potential. Although drain disinfection may be necessary in an outbreak scenario, we believe establishing the right frequency and duration of disinfection is critical for controlling sink drain biofilms and related pathogens, noting that inconsistent drain disinfection may come with a tradeoff of increased antimicrobial resistance.

The design of this study provided insights into immediate community shifts in the weeks following a single disinfection treatment. Future research is needed on dynamics during and after repeated applications over longer intervals, especially when a recommended treatment frequency schedule has been established. Additionally, larger-scale studies are needed to generalize findings, and analysis of clinical isolates could further relate microbial insights to clinical risk. Finally, our three-week follow-up may not have fully captured biofilm community stabilization, and it is unknown how long the elevated antimicrobial resistance and community shifts would have persisted. Despite these limitations, our results highlight key mechanisms by which disinfection treatment can reshape sink biofilm communities and potentially increase antimicrobial resistance risk. This study lays the foundation for future work exploring alternatives to HAI strategies beyond disinfection. A variety of methods have been attempted for drain biofilm removal, including pipe heating/sonication, boiling water flushes, and even pipe removal and replacement, although these approaches are often costly, time-consuming, and short-term. Alternatives include exploring variations in sink design, such as utilizing different drainpipe materials, using germicidal ultraviolet light,[50] and even introducing sinkless rooms,[51] or testing probiotic-based interventions to outcompete pathogens in the sink drain.[52,53] Ultimately, our findings underscore the need for infection control strategies that effectively manage sink biofilm dynamics, but also reduce conditions or pressures that drive the emergence and spread of antimicrobial resistance.

Methods

Sample collection

The study was conducted on a single floor (constructed 2009) focused on the care of patients with hematologic malignancies, particularly those with hematopoietic stem cell transplants, at Yale New

Haven Hospital in New Haven, CT, USA. Twelve treated sinks and seven untreated sinks were included in the study. Treatment consisted of one application of disinfectant to sink drains, described below. Of the treated sinks, six sinks were in patient rooms (P1, P2, P3, P4, P5, P6), and six sinks were in the hallway directly outside patient rooms and in patient care areas (H1, H2, H3, H4, H5, H6). All sinks were handicap sinks of the same make and model (Chicago Faucets automatic model 116.517.AB.1). Treated sinks were sampled at three timepoints over two weeks prior to treatment and ten timepoints over three weeks after, while the seven untreated sinks were primarily sampled on the final two sampling days. As part of routine hospital protocol, all sinks were subjected to daily cleaning of outer surfaces including the counter and sink bowl with either a hydrogen peroxide or bleach-based disinfectant.

The disinfectant used in this study was Virasept (EcoLab), a product approved by the United States Environmental Protection Agency for drain disinfection in 2020. Active ingredients include 3.13% hydrogen peroxide, 0.099% octanoic acid, and 0.05% peroxyacetic acid. Virasept was applied as directed with the associated foamer, ensuring sufficient contact time of ingredients with vertical pipe biofilms. The foam was injected into the drain until foam began spilling over the drain cover, about 60 mL per sink. The disinfectant was left to incubate for five minutes, with additional foam applied if it started to drain. Sinks were not used during incubation and electronic faucets were prevented from activating. After five minutes, the sinks were flushed for at least 45 seconds, until there was no visible disinfectant present.

Biofilm samples were collected using BD Liquid Amies Elution Swab (Eswab) Collection/Transport System. Sterile swabs were dipped in the Liquid Amies solution prior to sample collection. For drains, swabs were inserted approximately 7.6 cm and rotated across the pipe surface ten times (covering approx. 10 cm^2). Swabs were then reinserted into the Liquid Amies solution, sealed, and transported to the lab on ice to be processed within 24 hours.

Culture work

Swabs from all time points were vortexed in Liquid Amies solution to homogenize, then an aliquot of the solution was either plated or serially diluted in autoclaved tap water prior to plating. 50 µL aliquots of samples or dilutions were plated using the spread plate method with sterile spreader. Samples were cultured on KPC CHROMagar™ (“carbapenem-resistant bacteria”) and CHROMagar™ Orientation (“total bacteria”) plates. Plates (100 mm diameter) were made with 33 g/L chromagar media, and KPC supplement (400 mg/L) was added to the agar after cooling below 50°C. Sample dilutions were adjusted throughout the experiment (1x-100,000x) such that colonies were in a countable range. Colonies were counted after 24 hours of aerobic incubation at 37°C. Negative control plates spread with dilution water did not grow colonies.

DNA extraction and clean-up

123 swabs were extracted (Supplementary Table 1) using a Kingfisher Apex MagMax Microbiome TNA kit.[21] Briefly, swabs in Liquid Amies solution were bead-beaten for 15 minutes after adding lysis buffer and phenol-chloroform-isoamyl alcohol. The supernatant was removed after centrifugation and added into a 24-well plate with proteinase K for automated extraction with a Kingfisher Apex. After extraction, RNase A was added to a final concentration of 100 µg/mL and incubated at room temperature for 15 minutes prior to a column-based cleanup with the Genomic DNA Clean & Concentrator-10 kit (Zymo Research) to remove RNA.

Short-read sequencing and bioinformatics

119 sink drain biofilm samples along with two negative swab controls (unused swabs in liquid Amies) and two mock community positive controls (Zymo Research, ZymoBIOMICS Microbial Community Standard, cat #D6300) were sequenced at the Yale Center for Genomic Analysis (YCGA). YCGA completed the library preparation for 150 bp paired-end metagenomic shotgun sequencing at their facility then sequenced at a depth of 60 million reads per sample on the Illumina Novaseq 6000.

Illumina adapters were trimmed with cutadapt then data was prepared for processing using the Anvi'o Snakemake pipeline (version 8).[54,55] Within Anvi'o, KrakenUniq was used to classify taxonomy using the KrakenUniq MicrobialDB database which contains sequences from the NCBI RefSeq database including bacteria, archaea, and viruses, and the human reference genome.[56] Reads from each sample were individually assembled into contigs with a minimum length of 500 bp using Megahit.[57] Prodigal was then used to convert the contigs from DNA to protein,[58] then aligned to the CARD database with RGI to annotate ARGs.[59] For functional analysis, the assembled contigs were first removed from Anvi'o then binned with metabat2 before importing back into Anvi'o.[60] All data was exported into R for further analysis.

All samples generated sequencing data with a median of 47.6 million reads (range 28.2 to 113.1 million reads). Reads that could not be assigned at the Family level or higher were discarded. Taxa with a combined total of less than 1200 reads (0.005% of the median reads from all samples) were removed.[61,62] To determine if a taxon was a contaminant, a ratio of the relative abundance in the negative controls to the relative abundance in biological samples was computed. If the ratio was greater than 10 in >90% of samples, it was deemed a contaminant and removed from the dataset. Contaminants were visually inspected, and taxa that followed abundance patterns consistent with disinfection and regrowth were retained as true signal (e.g. Acidovorax). 16 taxa were labeled as a contaminant and were removed. After removal of reads unassigned to at least the family level and removal of contaminants, there was a median of 24.4 million reads per sample (range 11.4 million to 65.3 million reads, Supplementary Figure 12). The number of reads generated from the negative controls were not significantly different from the biofilm samples (Supplementary Figure 13A), and although the taxonomic members were similar to true samples, the community structure of the controls did not match the true samples (Supplementary Figure 13B). Negative controls had undetectable DNA concentrations via Qubit Fluorometer (Thermo Fisher Scientific), while the untreated sinks had DNA concentrations between 14.1 ng/µL and 21.2 ng/µL. Therefore we suspect the high number of reads in negative controls was due to well-to-well contamination from samples, which has been documented in prior studies to specifically impact low-biomass samples.[63] Rarefaction curves were generated for all samples to evaluate whether sequencing depth influenced observed diversity. As the curves indicated adequate coverage, we proceeded without rarefying the data (Supplementary Figure 5B). All subsequent analyses on the shotgun metagenomic data was done on taxa agglomerated at the Genus level.

To estimate the number of shotgun sequencing reads mapping to each ARG in each sample, we combined ARG annotations with contig-level coverage data. Specifically, contig coverage values were merged with ARG gene coordinates, and the length of each ARG was calculated from its start and stop positions. The number of reads per ARG was then estimated by multiplying the ARG length by the

contig coverage and dividing by the average sequencing read length (150 bp). This approach provides an approximate read count for each ARG, facilitating downstream abundance analyses.

Long-read sequencing and bioinformatics

24 samples were multiplexed and submitted for HiFi long-read sequencing using the PacBio Revio at the Keck Microarray Shared Resource at Yale University. MAGs were generated exclusively from PacBio long-read sequencing data. Raw reads were assembled using metaFlye with the “meta” and “pacbio” flags.[64] Samples were processed using PacBio’s HiFi MAG pipeline v2.0. Contigs greater than 500 kb with greater than 93% completion were considered final MAGs. The remaining long contigs were pooled with short contigs (<500 kb) and underwent binning with both SemiBin2 and MetaBat2.[60,65] The resulting bins were compared and merged using DasTool,[66] then filtered with CheckM2 for > 70% completeness,[67] <10% contamination, and <20 contigs. All final complete MAGs were taxonomically classified using GTDB-Tk which generated final FASTA files and phylogenetic trees.[68] For chromosomal antibiotic resistance gene annotation, Prodigal was used to predict the protein-coding genes from the final MAGs.[58] Finally, RGI plus CARD was used in Strict mode to assign antibiotic resistance genes to the predicted proteins.[59] ARGs with a >75% percent identity and >40% coverage were retained. We recovered an average of 11.0 ± 3.7 MAGs per sample.

The relative abundance of chromosomal MAGs was calculated as coverage multiplied by MAG length divided by the total number of bases in the sample. To determine ARG coverage, we used the length of the ARG and multiplied by the coverage of the MAG. ARG coverage was then divided by total number of bases in the sample to get ARG relative abundance. The ARG categories were first separated using the “Resistance Mechanism” output from CARD, and then further classified into specific resistances (i.e. fosfomycin) using prior work.[42] To examine non-chromosomal ARGs, the unbinned contigs were annotated similarly to the complete MAGs with Prodigal followed by RGI plus CARD. Similar to prior environmental long-read sequencing work, we used PlasFlow to flag the unbinned contigs as either chromosome or plasmid.[69] Final results were combined and loaded into R for data analysis.

Data analysis

All data analysis was completed using R and Rstudio (version 4.5.0, 2025.05.0+496 respectively). All the data analysis code is in the GitHub repository [https://github.com/gersteinlab/sinkbiofilm].[70] The GitHub includes code and processed data used for analysis, consisting of: metadata including colony counts from culture data, taxonomy and ARG tables from the shotgun metagenomics data, ARG information for the PacBio long-read sequencing, contig coverage of the MAGs, plasmid coverage, scores, and ARG information from the long-read sequencing. Phyloseq (version 1.42.0) was used to analyze the short-read shotgun metagenomics data, including the negative controls and mock community positive controls, as well as the long-read sequencing data. Raup-Crick null model analysis based on Bray-Curtis dissimilarity was performed using the iCAMP package (version 1.5.12) to assess whether observed community dissimilarity deviated from null expectations. All stacked barplots were generated using *microshades* (version 1.11).[71] MaAslin3 was used to evaluate differentially abundant taxa between after and regrowth compared to the before phase.[72] The fixed effect was the experimental phase, while the random effects included both the specific sink and the sink location (i.e. hallway or patient) as they were not the main focus of this analysis. Alpha diversity of ARGs was calculated at the gene-level, with each unique ARG treated as a discrete unit.

Statistics & Reproducibility

All data analysis and statistics were completed in R. The vegan R package version 2.6.4 and *rstatix* version 0.7.2 were used for all statistical analyses. The Shapiro-Wilk test was used to determine normality. A Kruskal-Wallis test was used to test for significant differences between the experimental phases and relative abundance of specific taxonomy, followed by a pairwise two-sided Wilcoxon Rank Sum test with false discovery rate (FDR) correction. No statistical method was used to predetermine sample size. No data, outside of the filtered sequencing data described above, were excluded from the analyses. The experiments were not randomized. The Investigators were not blinded to allocation during experiments and outcome assessment. This study was deemed exempt from review by Yale University's Institutional Review Board (Study #2000036758).

Data Availability

Sequencing data were deposited in NCBI SRA (PRJNA1310651). Both the shotgun metagenomic data and long-read metagenomic data generated in this study have been deposited in the NCBI SRA database under accession code "PRJNA1310651 [https://www.ncbi.nlm.nih.gov/bioproject/?term=(PRJNA1310651)]". All data are available. The processed data for both the short- and long-read sequencing are available on Github [https://github.com/gersteinlab/sinkbiofilm].[70] Source data are provided with this paper.

Code Availability

All custom codes used in the reported analyses are available on the GitHub page [https://github.com/gersteinlab/sinkbiofilm].[70] All software and package versions are detailed at the top of each code script.

References

1. Nelson, R. E. *et al.* National Estimates of Healthcare Costs Associated With Multidrug-Resistant Bacterial Infections Among Hospitalized Patients in the United States. *Clinical Infectious Diseases* **72**, S17–S26 (2021).
2. Hayward, C. *et al.* Drinking water plumbing systems are a hot spot for antimicrobial-resistant pathogens. *Journal of Hospital Infection* **159**, 62–70 (2025).
3. Bourdin, T. *et al.* Disinfection of sink drains to reduce a source of three opportunistic pathogens, during Serratia marcescens clusters in a neonatal intensive care unit. *PLoS ONE* **19**, e0304378 (2024).

4. Mathers, A. J. *et al.* Klebsiella pneumoniae carbapenemase (KPC)-producing K. pneumoniae at a single institution: insights into endemicity from whole-genome sequencing. *Antimicrob Agents Chemother* **59**, 1656–1663 (2015).
5. Leitner, E. *et al.* Contaminated Handwashing Sinks as the Source of a Clonal Outbreak of KPC-2-Producing Klebsiella oxytoca on a Hematology Ward. *Antimicrob Agents Chemother* **59**, 714–716 (2015).
6. Carling, P. C. Wastewater drains: epidemiology and interventions in 23 carbapenem-resistant organism outbreaks. *Infect. Control Hosp. Epidemiol.* **39**, 972–979 (2018).
7. Parkes, L. O. & Hota, S. S. Sink-Related Outbreaks and Mitigation Strategies in Healthcare Facilities. *Curr Infect Dis Rep* **20**, 42 (2018).
8. Kotay, S. M. *et al.* Droplet- Rather than Aerosol-Mediated Dispersion Is the Primary Mechanism of Bacterial Transmission from Contaminated Hand-Washing Sink Traps. *Appl Environ Microbiol* **85**, e01997-18 (2019).
9. Hausner, M. & Wuertz, S. High rates of conjugation in bacterial biofilms as determined by quantitative in situ analysis. *Appl Environ Microbiol* **65**, 3710–3713 (1999).
10. *WHO Bacterial Priority Pathogens List 2024: Bacterial Pathogens of Public Health Importance, to Guide Research, Development, and Strategies to Prevent and Control Antimicrobial Resistance*. (World Health Organization, Geneva, 2024).
11. Centers for Disease Control and Prevention (U.S.). *Antibiotic Resistance Threats in the United States, 2019*. https://stacks.cdc.gov/view/cdc/82532 (2019) doi:10.15620/cdc:82532.
12. Jones, L. D. *et al.* Effectiveness of foam disinfectants in reducing sink-drain gram-negative bacterial colonization. *Infect. Control Hosp. Epidemiol.* **41**, 280–285 (2020).
13. Warren, B. G. *et al.* Efficacy of a foamed disinfectant in reducing pathogen contamination in renovated inpatient in-room sinks: a randomized controlled trial. *Infect. Control Hosp. Epidemiol.* **47**, 13–19 (2026).

14. Newcomer, E. P. *et al.* The effects of a prospective sink environmental hygiene intervention on Pseudomonas aeruginosa and Stenotrophomonas maltophilia burden in hospital sinks. *eBioMedicine* **116**, 105772 (2025).
15. Buchan, B. W. *et al.* Effectiveness of a hydrogen peroxide foam against bleach for the disinfection of sink drains. *Infect Control Hosp Epidemiol* **40**, 724–726 (2019).
16. Ledwoch, K., Robertson, A., Lauran, J., Norville, P. & Maillard, J.-Y. It's a trap! The development of a versatile drain biofilm model and its susceptibility to disinfection. *J Hosp Infect* **106**, 757–764 (2020).
17. Short, F. L. *et al.* Benzalkonium chloride antagonises aminoglycoside antibiotics and promotes evolution of resistance. *EBioMedicine* **73**, 103653 (2021).
18. Kim, M. *et al.* Widely Used Benzalkonium Chloride Disinfectants Can Promote Antibiotic Resistance. *Appl Environ Microbiol* **84**, e01201-18 (2018).
19. Butler, J., Kelly, S. D., Muddiman, K. J., Besinis, A. & Upton, M. Hospital sink traps as a potential source of the emerging multidrug-resistant pathogen Cupriavidus pauculus: characterization and draft genome sequence of strain MF1. *J Med Microbiol* **71**, 001501 (2022).
20. Ryan, M. P., Sevjahova, L., Gorman, R. & White, S. The Emergence of the Genus Comamonas as Important Opportunistic Pathogens. *Pathogens* **11**, 1032 (2022).
21. Healy, H. G. *et al.* Bacterial Recolonization of Hospital Sink Biofilms. *Journal of Hospital Infection* S0195670125001616 (2025) doi:10.1016/j.jhin.2025.05.013.
22. Lunder, T., Eversen, Ø., Holstad, G. & Håstein, T. 'Winter ulcer' in the Atlantic salmon Salmo salar. Pathological and bacteriological investigations and transmission experiments. *Dis. Aquat. Org.* **23**, 39–49 (1995).
23. Zuckerberg ID, C. CZ ID Pathogen List. https://czid.org/pathogen_list (2025).
24. Shapiro, K. *et al.* Healthcare-Associated Infections Caused by Mycolicibacterium neoaurum. *Emerg Infect Dis* **29**, 1516–1523 (2023).
25. Grabowski, M. *et al.* Characterizations of handwashing sink activities in a single hospital medical intensive care unit. *Journal of Hospital Infection* **100**, e115–e122 (2018).

26. Kaviani, R., Pouladi, I., Niakan, M. & Mirnejad, R. Molecular Detection of Adefg Efflux Pump Genes and their Contribution to Antibiotic Resistance in Acinetobacter baumannii Clinical Isolates. *Rep Biochem Mol Biol* **8**, 413–418 (2020).
27. Costa, S. S., Viveiros, M., Amaral, L. & Couto, I. Multidrug Efflux Pumps in Staphylococcus aureus: an Update. *Open Microbiol J* **7**, 59–71 (2013).
28. Cox, G., Stogios, P. J., Savchenko, A. & Wright, G. D. Structural and Molecular Basis for Resistance to Aminoglycoside Antibiotics by the Adenylyltransferase ANT(2″)-Ia. *mBio* **6**, e02180-14 (2015).
29. Iovleva, A. *et al.* Reduced ceftazidime and ertapenem susceptibility due to production of OXA-2 in Klebsiella pneumoniae ST258. *J Antimicrob Chemother* **74**, 2203–2208 (2019).
30. Calderón-Franco, D., Van Loosdrecht, M. C. M., Abeel, T. & Weissbrodt, D. G. Free-floating extracellular DNA: Systematic profiling of mobile genetic elements and antibiotic resistance from wastewater. *Water Research* **189**, 116592 (2021).
31. Lin, J.-N., Lai, C.-H., Yang, C.-H., Huang, Y.-H. & Lin, H.-H. *Elizabethkingia bruuniana* Infections in Humans, Taiwan, 2005–2017. *Emerg. Infect. Dis.* **25**, 1412–1414 (2019).
32. Kubota, H. *et al.* Emergence of *Phytobacter diazotrophicus* carrying an IncA/C_2 plasmid harboring bla_{NDM-1} in Tokyo, Japan. *mSphere* **8**, e00147-23 (2023).
33. Jia, J. *et al.* Pseudomonas glycinae sp. nov. isolated from the soybean rhizosphere. *Microbiologyopen* **9**, e1101 (2020).
34. Abe, R. *et al.* Characterization of the Plasmidome Encoding Carbapenemase and Mechanisms for Dissemination of Carbapenem-Resistant *Enterobacteriaceae*. *mSystems* **5**, e00759-20 (2020).
35. Black, C. A. *et al.* Predominance of Non-carbapenemase Producing Carbapenem-Resistant Enterobacterales in South Texas. *Front Microbiol* **11**, 623574 (2020).
36. Akinbobola, A. B., Sherry, L., Mckay, W. G., Ramage, G. & Williams, C. Tolerance of Pseudomonas aeruginosa in in-vitro biofilms to high-level peracetic acid disinfection. *J Hosp Infect* **97**, 162–168 (2017).

37. Sukhum, K. V. *et al.* Antibiotic-resistant organisms establish reservoirs in new hospital built environments and are related to patient blood infection isolates. *Commun Med* **2**, 62 (2022).
38. Snell, L. B. *et al.* The drainome: longitudinal metagenomic characterization of wastewater from hospital ward sinks to characterize the microbiome and resistome and to assess the effects of decontamination interventions. *Journal of Hospital Infection* **153**, 55–62 (2024).
39. Chen, X. *et al.* PafS Containing GGDEF-Domain Regulates Life Activities of Pseudomonas glycinae MS82. *Microorganisms* **10**, 2342 (2022).
40. Zeng, W. *et al.* Insights into the production of extracellular polymeric substances of *Cupriavidus pauculus* 1490 under the stimulation of heavy metal ions. *RSC Adv.* **10**, 20385–20394 (2020).
41. Gaurav, A., Bakht, P., Saini, M., Pandey, S. & Pathania, R. Role of bacterial efflux pumps in antibiotic resistance, virulence, and strategies to discover novel efflux pump inhibitors. *Microbiology (Reading)* **169**, 001333 (2023).
42. Shao, X. *et al.* The transcriptional regulators of virulence for Pseudomonas aeruginosa: Therapeutic opportunity and preventive potential of its clinical infections. *Genes Dis* **10**, 2049–2063 (2023).
43. Antunes, N. T. *et al.* Class D β-lactamases: are they all carbapenemases? *Antimicrob Agents Chemother* **58**, 2119–2125 (2014).
44. van Duin, D. *et al.* Molecular and clinical epidemiology of carbapenem-resistant Enterobacterales in the USA (CRACKLE-2): a prospective cohort study. *Lancet Infect Dis* **20**, 731–741 (2020).
45. Teo, J. Q.-M. *et al.* Genomic characterization of carbapenem-non-susceptible *Pseudomonas aeruginosa* in Singapore. *Emerging Microbes & Infections* **10**, 1706–1716 (2021).
46. Gao, X. *et al.* Prolonged Exposure to Environmentally Relevant Concentrations of Chlorine Induces Heritable Antimicrobial Resistance in Disinfection Residual *Pseudomonas aeruginosa*. *Environ. Sci. Technol.* **59**, 3895–3905 (2025).
47. Zhang, Y. *et al.* Overproduction of efflux pumps caused reduced susceptibility to carbapenem under consecutive imipenem-selected stress in Acinetobacter baumannii. *Infect Drug Resist* **11**, 457–467 (2017).

48. Rasheed, H. *et al.* Discrepancies between phenotypic and genotypic identification methods of antibiotic resistant genes harboring Staphylococcus aureus. *Microbial Pathogenesis* **184**, 106342 (2023).
49. Davies, T. J. *et al.* Reconciling the Potentially Irreconcilable? Genotypic and Phenotypic Amoxicillin-Clavulanate Resistance in *Escherichia coli*. *Antimicrob Agents Chemother* **64**, e02026-19 (2020).
50. Norville, P., Wilkinson, M. A. C., Shale, E., Holden, E. & Garvey, M. The effect of continuous UV-C disinfection on microbial contamination of a handwash basin. *Journal of Hospital Infection* S0195670125002282 (2025) doi:10.1016/j.jhin.2025.07.012.
51. Hopman, J. *et al.* Reduced rate of intensive care unit acquired gram-negative bacilli after removal of sinks and introduction of 'water-free' patient care. *Antimicrob Resist Infect Control* **6**, 59 (2017).
52. Hegarty, B. Making waves: Intelligent phage cocktail design, a pathway to precise microbial control in water systems. *Water Res* **268**, 122594 (2025).
53. Denkel, L. A. *et al.* Can probiotics trigger a paradigm shift for cleaning healthcare environments? A narrative review. *Antimicrob Resist Infect Control* **13**, 119 (2024).
54. Martin, M. Cutadapt removes adapter sequences from high-throughput sequencing reads. *EMBnet j.* **17**, 10 (2011).
55. Eren, A. M. *et al.* Community-led, integrated, reproducible multi-omics with anvi'o. *Nat Microbiol* **6**, 3–6 (2020).
56. Breitwieser, F. P., Baker, D. N. & Salzberg, S. L. KrakenUniq: confident and fast metagenomics classification using unique k-mer counts. *Genome Biol* **19**, 198 (2018).
57. Li, D., Liu, C.-M., Luo, R., Sadakane, K. & Lam, T.-W. MEGAHIT: an ultra-fast single-node solution for large and complex metagenomics assembly via succinct *de Bruijn* graph. *Bioinformatics* **31**, 1674–1676 (2015).
58. Hyatt, D. *et al.* Prodigal: prokaryotic gene recognition and translation initiation site identification. *BMC Bioinformatics* **11**, 119 (2010).

59. Alcock, B. P. *et al.* CARD 2023: expanded curation, support for machine learning, and resistome prediction at the Comprehensive Antibiotic Resistance Database. *Nucleic Acids Res* **51**, D690–D699 (2023).
60. Kang, D. D. *et al.* MetaBAT 2: an adaptive binning algorithm for robust and efficient genome reconstruction from metagenome assemblies. *PeerJ* **7**, e7359 (2019).
61. Poussin, C. *et al.* Crowdsourced benchmarking of taxonomic metagenome profilers: lessons learned from the sbv IMPROVER Microbiomics challenge. *BMC Genomics* **23**, (2022).
62. Luhung, I. *et al.* Experimental parameters defining ultra-low biomass bioaerosol analysis. *npj Biofilms Microbiomes* **7**, (2021).
63. Walker, A. W. A Lot on Your Plate? Well-to-Well Contamination as an Additional Confounder in Microbiome Sequence Analyses. *mSystems* **4**, e00362-19 (2019).
64. Kolmogorov, M. *et al.* metaFlye: scalable long-read metagenome assembly using repeat graphs. *Nat Methods* **17**, 1103–1110 (2020).
65. Pan, S., Zhao, X.-M. & Coelho, L. P. SemiBin2: self-supervised contrastive learning leads to better MAGs for short- and long-read sequencing. *Bioinformatics* **39**, i21–i29 (2023).
66. Sieber, C. M. K. *et al.* Recovery of genomes from metagenomes via a dereplication, aggregation and scoring strategy. *Nat Microbiol* **3**, 836–843 (2018).
67. Chklovski, A., Parks, D. H., Woodcroft, B. J. & Tyson, G. W. CheckM2: a rapid, scalable and accurate tool for assessing microbial genome quality using machine learning. *Nat Methods* **20**, 1203–1212 (2023).
68. Chaumeil, P.-A., Mussig, A. J., Hugenholtz, P. & Parks, D. H. GTDB-Tk: a toolkit to classify genomes with the Genome Taxonomy Database. *Bioinformatics* **36**, 1925–1927 (2020).
69. Krawczyk, P. S., Lipinski, L. & Dziembowski, A. PlasFlow: predicting plasmid sequences in metagenomic data using genome signatures. *Nucleic Acids Research* **46**, e35–e35 (2018).
70. Kate Bowie. gersteinlab/sinkbiofilm: Sink Drain Biofilm manuscript version. Zenodo https://doi.org/10.5281/ZENODO.19702190 (2026).

71. Dahl, E. M., Neer, E., Bowie, K. R., Leung, E. T. & Karstens, L. microshades : An R Package for Improving Color Accessibility and Organization of Microbiome Data. *Microbiology Resource Announcements* **11**, (2022).

72. Nickols, W. A. *et al.* MaAsLin 3: Refining and extending generalized multivariable linear models for meta-omic association discovery. Preprint at https://doi.org/10.1101/2024.12.13.628459 (2024).

Acknowledgements
We thank the YNHH nursing staff and patients on the study floor for accommodating our sampling campaign. We are grateful to the HIPSTER consortia, especially helpful discussions with and support from Lucien Dieter, Trini Mathew, Jamie Trumpler, David Peaper, and Windy Tanner.

Funding
This publication was supported by the Centers for Disease Control and Prevention (CDC) of the US Department of Health and Human Services (HHS) as part of a financial assistance award totaling $3,014,045.50 with 100% funded by the CDC/HHS. The contents are those of the author(s) and do not necessarily represent the official views of, nor an endorsement, by the CDC/HHS or the US Government. Research reported in this publication was also supported by the National Institute of General Medical Sciences of the National Institutes of Health under Award Number 1S10OD030363-01A1. The Yale Center for Genome Analysis and Keck Microarray Shared Resource at Yale University provided the PacBio sequencing services and is funded in part by the National Institutes of Health instrument grant 1S10OD028669-01. This work was also supported by the Yale Institute for Biospheric Studies Gaylord Donnelley Postdoctoral Environmental Fellowship (H.G.H.). and the National Library of Medicine (NLM) training grant T15LM [T15LM007056], which supports the Biomedical Informatics and Data Science training program at Yale University (K.R.B.).

Author Information
Authors and Affiliations
Department of Chemical and Environmental Engineering, Yale University, New Haven, CT, USA
Kate R. Bowie, Irvan Luhung, Taylor Burke & Jordan Peccia

Department of Molecular Biophysics and Biochemistry, Yale University, New Haven, CT, USA
Kate R. Bowie, Mark B. Gerstein

Department of Internal Medicine, Section of Infectious Diseases, Yale School of Medicine, New Haven, CT, USA
Scott C. Roberts, Richard A. Martinello

Department of Infection Prevention, Yale New Haven Health, New Haven, CT, USA
Scott C. Roberts, Richard A. Martinello

Department of Pediatrics, Yale School of Medicine, New Haven, CT, USA
Richard A. Martinello

Program in Computational Biology & Bioinformatics, Yale University, New Haven, CT, USA
Mark B. Gerstein

Department of Computer Science, Yale University, New Haven, CT, USA
Mark B. Gerstein

Department of Statistics & Data Science, Yale University, New Haven, CT, USA
Mark B. Gerstein

Harvard T.H. Chan School of Public Health, Harvard University, Boston, Massachusetts
Hannah Greenwald Healy

Author Contributions Statement

H.G.H. conceptualized and designed the study. K.R.B., H.G.H., I.L., S.C.R. coordinated sample collection, and K.R.B., H.G.H., and I.L. collected samples and conducted laboratory analysis. K.R.B. processed and analyzed all sequencing data. K.R.B., I.L., and T.B. generated all figures and associated code. K.R.B. and H.G.H. wrote the original draft of the manuscript. R.A.M., J.L.P., M.B.G., and H.G.H contributed to funding acquisition. All authors provided feedback on the analysis and manuscript draft.

Ethics Declarations

Competing Interests

The authors declare no competing interests.

Figure Captions

Figure 1. Overview of experimental design and sampling scheme across experimental phases. Schematic of sink drain sampling timeline including the methods used for data generation.

Figure 2. Total and carbapenem-resistant bacteria cultured from sink drain biofilms before and after disinfection treatment.
(A) Cultured total bacteria (n = 12 samples per day) and (B) carbapenem-resistant bacteria from sink drain biofilms by study day, where drains were disinfected on Day 15 (n = 12 samples per day). Sink rooms are designated with “P” for patient or “H” for hallway. Sampling days were separated into

experimental phases: before (days 1-15B, B = before), after (days 15D-19, D = disinfection) and regrowth (days 20-36). Dashed blue lines represent the median CFU/cm^2 of the first three timepoints ('before' phase) for each media type, and x-axis sampling days are not to scale. (C) Comparison of cultured viable bacteria from treated (red; n = 12 samples) and untreated (blue; n = 7 samples) sink drain biofilms cultured during the regrowth phase from total and (D) carbapenem-resistant bacteria (p = 0.002, two-sided Wilcoxon Rank Sum test). Box edges of all plots correspond to the first quartile, median, and third quartile. Whiskers extend from the edge to the largest and smallest values no further than 1.5× the interquartile range from the edge. Data beyond the whiskers are considered outliers and plotted individually. Source data are provided as a Source Data file.

Figure 3. Shotgun metagenomics reveals enrichment of *Cupriavidus* and *Pseudomonas* and reduced diversity in sink drain biofilms following disinfection treatment.
(A) Stacked relative abundance bar plot at the genus level of the sink biofilm sample microbial communities separated into experimental phases (before, after, and regrowth after disinfection treatment). (B) Stacked bar plot of the untreated control sink drain biofilm communities with similarity to the samples before treatment. (C) Boxplot of relative abundance of *Cupriavidus* across experimental phases (Kruskal-Wallis; post-hoc two-sided Wilcoxon Rank Sum test with FDR correction, n = 36 samples per phase). (D) Boxplot of relative abundance of *Pseudomonas* across the experimental phases in order (before, after, regrowth), faceted into patient and hallway sink drain biofilms (Kruskal-Wallis; post-hoc two-sided Wilcoxon Rank Sum test with FDR correction, n = 36 samples per phase). (E) Boxplot of the Inverse Simpson index across experimental phases with p values displayed above brackets (Kruskal-Wallis; post-hoc two-sided Wilcoxon Rank Sum test with FDR correction, n = 36 samples per phase). Box edges of all plots correspond to the first quartile, median, and third quartile. Whiskers extend from the edge to the largest and smallest values no further than 1.5× the interquartile range from the edge. Data beyond the whiskers are considered outliers and plotted individually. (F) Volcano plot comparing microbial abundance in the before vs. regrowth phases (n = 36 samples per phase). The x-axis shows MaAsLin3 effect size, and the Y-axis shows significance (-log10 q-value). Each point represents a genus significantly associated with the transition from the baseline (before) to the regrowth phase. Genera with positive (red) effect sizes are more abundant in the regrowth phase, while those with negative (green) effect sizes are more abundant before treatment. Point size indicates mean relative abundance across samples, and the six genera with the lowest p-values were labeled. Source data for each panel are provided as a Source Data file.

Figure 4.Long-read metagenomics demonstrated an increased relative abundance of ARG-carrying MAGs in sink drain biofilms post-treatment, with multidrug efflux pumps as the predominant resistance mechanism.
(A) Boxplot of the total RPKM of ARGs annotated in the shotgun metagenomic sequencing data by experimental phase, with p values displayed above brackets (Kruskal-Wallis; post-hoc two-sided Wilcoxon Rank Sum test with FDR correction, n = 36 samples per phase). (B) Boxplot of the relative abundance of MAGs with ARGs before treatment and in the regrowth phase (two-sided Wilcoxon Rank Sum test, n = 12 samples per phase). (C) Heatmap shows number of taxa with the ARG category of interest, described in Supplementary Table 7. MAGs were collapsed at the species level and were subset by those with >2 detections. Color intensity reflects the number of times the species-ARG pair

was detected across samples. (D) Percent change of the detected efflux pump-associated ARGs found in MAGs. Green represents ARGs that were detected more frequently before treatment while red represents ARGs detected more frequently in the regrowth phase after disinfection treatment. (E) Boxplot demonstrating the number of plasmids before treatment and in regrowth (ns = not significant where p = 0.16, two-sided Wilcoxon Rank Sum test, n = 12 samples per phase). (F) Boxplot demonstrating the proportion of plasmids with carbapenemases before disinfection treatment and in regrowth (ns = not significant where p = 0.24, two-sided Wilcoxon Rank Sum test, n = 12 samples per phase). Box edges of all plots correspond to the first quartile, median, and third quartile. Whiskers extend from the edge to the largest and smallest values no further than 1.5× the interquartile range from the edge. Data beyond the whiskers are considered outliers and plotted individually. Source data are provided as a Source Data file.

This study informs disinfection strategies in clinical settings. Authors report that disinfection of sink drain biofilms initially reduced microbial load, followed by regrowth favouring bacteria enriched with multidrug efflux pumps.

Peer review information: *Nature Communications* thanks the anonymous reviewers for their contribution to the peer review of this work. A peer review file is available.

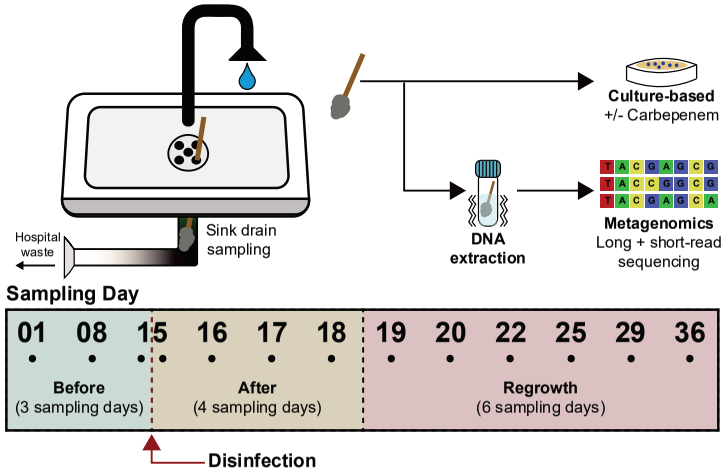

ARTICLE IN PRESS

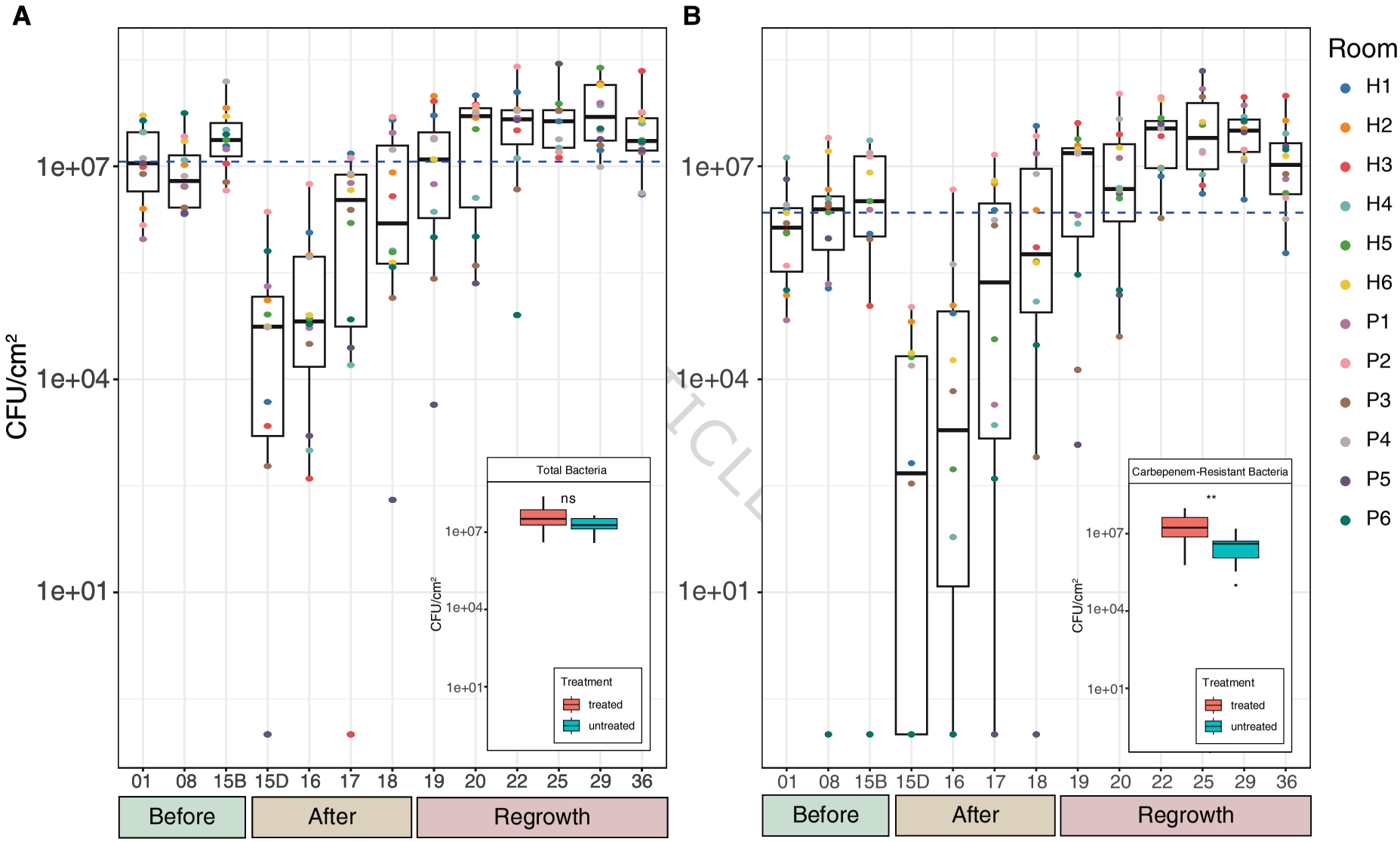

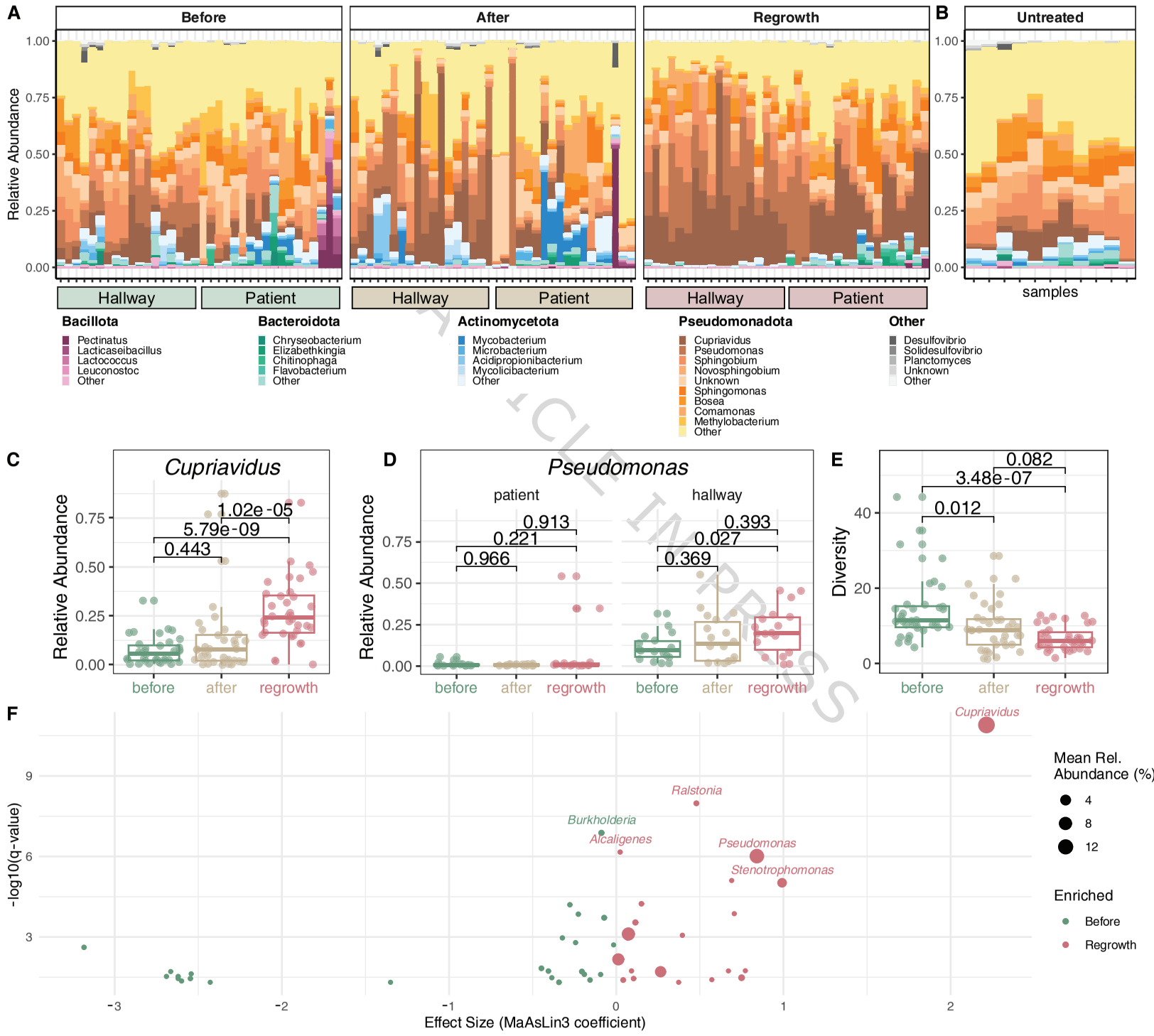

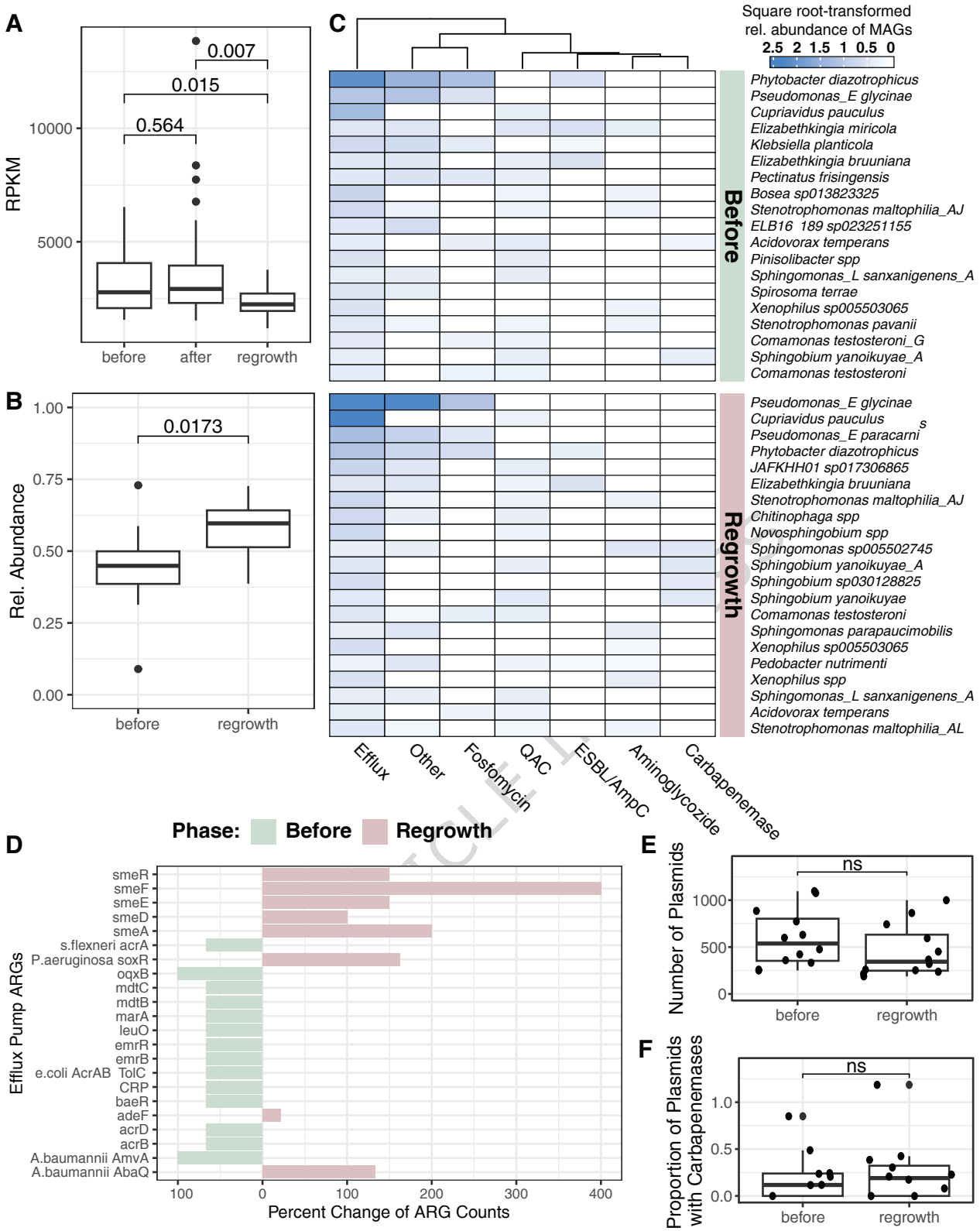
A
RPKM
10000
5000
0.007
0.015
0.564
before
after
regrowth
B
Rel. Abundance
1.00
0.75
0.50
0.25
0.00
0.0173
before
regrowth
C
Square root-transformed
rel. abundance of MAGs
2.5 2 1.5 1 0.5 0
Before
Phytobacter diazotrophicus
Pseudomonas_E glycinae
Cupriavidus pauculus
Elizabethkingia miricola
Klebsiella planticola
Elizabethkingia bruuniana
Pectinatus frisingensis
Bosea sp013823325
Stenotrophomonas maltophilia_AJ
ELB16 189 sp023251155
Acidovorax temperans
Pinisolibacter spp
Sphingomonas_L sanxanigenens_A
Spirosoma terrae
Xenophilus sp005503065
Stenotrophomonas pavanii
Comamonas testosteroni_G
Sphingobium yanoikuyae_A
Comamonas testosteroni
Regrowth
Pseudomonas_E glycinae
Cupriavidus pauculus
Pseudomonas_E paracarni
Phytobacter diazotrophicus
JAFKHH01 sp017306865
Elizabethkingia bruuniana
Stenotrophomonas maltophilia_AJ
Chitinophaga spp
Novosphingobium spp
Sphingomonas sp005502745
Sphingobium yanoikuyae_A
Sphingobium sp030128825
Sphingobium yanoikuyae
Comamonas testosteroni
Sphingomonas parapaucimobilis
Xenophilus sp005503065
Pedobacter nutrimenti
Xenophilus spp
Sphingomonas_L sanxanigenens_A
Acidovorax temperans
Stenotrophomonas maltophilia_AL
Efflux
Other
Fosfomycin
QAC
ESBL/AmpC
Aminoglycozide
Carbapenemase
D
Phase: Before Regrowth
Efflux Pump ARGs
smeR
smeF
smeE
smeD
smeA
s.flexneri acrA
P.aeruginosa soxR
oqxB
mdtC
mdtB
marA
leuO
emrR
emrB
e.coli AcrAB TolC
CRP
baeR
adeF
acrD
acrB
A.baumannii AmvA
A.baumannii AbaQ
100
0
100
200
300
400
Percent Change of ARG Counts
E
Number of Plasmids
1000
500
0
ns
before
regrowth
F
Proportion of Plasmids
with Carbapenemases
1.0
0.5
0.0
ns
before
regrowth